Front. Mech. Eng. 2013, 8(2): 109–117
DOI 10.1007/s11465-013-0252-z

RESEARCH ARTICLE

Jinxin LIU, Xuefeng CHEN, Zhengjia HE

Frequency domain active vibration control of a flexible plate based on neural networks

Abstract A neural-network (NN)-based active control system was proposed to reduce the low frequency noise radiation of the simply supported flexible plate. Feedback control system was built, in which neural network controller (NNC) and neural network identifier (NNI) were applied. Multi-frequency control in frequency domain was achieved by simulation through the NN-based control systems. A pre-testing experiment of the control system on a real simply supported plate was conducted. The NN-based control algorithm was shown to perform effectively. These works lay a solid foundation for the active vibration control of mechanical structures.

Keywords active vibration control (AVC), neural network (NN), low frequency noise, frequency domain control, multi-frequency control

1 Introduction

Active vibration control (AVC) technology has been developed for more than 30 years. Combining the vibration theory with the control theory, it has been widely applied in fields of civil engineering, aeronautics, astronautics, mechanical engineering and vehicle, etc. [1]. When referring to vibration control, the low frequency noise control problem is a hard bone that the conventional passive control or semi-active control methods fails to work. Fortunately, by energy consuming, AVC has the ability to solve this problem actively and effectively [2].

Actually, AVC is a complex control process and has many aspects to investigate, such as the control law, the sensors and actuators technology, the transfer path analysis (TPA) [3], the nonlinearity and time-delay of the system. Among them, the control law is the most important and essential one. Many investigations have reported on control laws, including the linear quadratic regulator (LQR) method [4], the independence modal space control (IMSC) [5], the robust H_∞ control [6] and positive position feedback (PPF) [7], etc. As the methods above mainly require precisely modeling, the intelligent methods, such as neural network (NN) and genetic algorithm (GA), have greater potential.

Intelligent methods receive many approvals, as they need no precisely modeling and have strong ability to approximate the nonlinear system. NN, a kind of network method that imitates the neurons and neural networks of intelligent creatures, is one of the most potential intelligent methods. Large amount of publications of NN on active control and system identification were presented. Early literatures of NN-based active vibration control stem from the series research of Rao et al. [8–10]. They outlined the structural identification and robust control method used for smart structures and then applied the NN-based AVC algorithm to smart structures using adaptive learning rate algorithm and adaptive neurons. Finally, they conducted the experiments on cantilever plate through i80170NX chip. In the past decennium, Jha and He [11] introduced an active control experiment on smart structure using NN-based one-step ahead prediction method. Jnifene and Andrews [12], Kumar et al. [13] and Madkour et al. [14] compared some others control methods, such as LQR, fuzzy logic control (FLC) and GA with NN and showed the advantages of NN. What's more, Abiyev and Kaynak [15], Pan and Wang [16] worked on nonlinear system by fuzzy wavelet NN and fuzzy NN sliding-mode control, respectively. In 2012, Zhang et al. [17] firstly proposed dynamic frequency characteristic active control (DFCAC) method. It stressed to drive the controlled system to the optimal vibration condition using NN method, which broke the deadlock of "only-decrease" in active vibration control.

The published papers mainly applied the control in time domain, which, in some situation, shows the disadvantages of low efficiency and being too sensitive to noise. In

Received December 15, 2012; accepted April 12, 2013

Jinxin LIU, Xuefeng CHEN (✉), Zhengjia HE
Key State Laboratory of Manufacturing System Engineering, Xi'an Jiaotong University, Xi'an 710049, China
E-mail: Chenxf@mail.xjtu.edu.cn

addition, time domain control is a kind of wide band control that cannot focus on some certain frequency points. Thus, NN-based frequency domain active control methods were studied. Specifically, we stress the following two points:

1) Frequency domain control

That means we will collect a signal sequence from the structure and then transfer it into frequency domain to construct the target function and finally exert the control force.

2) Multi-frequency control

That means we will control more than one spectrum peak at the same time by one actuator. In fact, every frequency peak is precisely taken into account in the target function.

2 Modeling

2.1 Finite element method (FEM) analysis

The simply supported flexible plate, which is an infinite degree of freedom (DOF) objective, is reduced into finite DOF model by FEM. The plate is divided into rectangle element as shown in Fig. 1(a). Figure 1(b) shows the ith element of the plate, which has four nodes (node 1, 2, 3, 4). The elements are assumed to connect with each other by nodes. For a transverse vibration plate, each node has three DOFs. They are a moving DOF along the axis of z^{ei} (ω in Fig. 1(b)) and rotating DOFs round the axis of x^{ei} and y^{ei} (θ_x and θ_y in Fig. 1(b)).

The element mass matrix $[\boldsymbol{M}^{ei}]$ and the element stiffness matrix $[\boldsymbol{K}^{ei}]$ can be constructed by element division and element analysis. They are (12 × 12) dimension matrixes, where e indicates *element* and i indicates the ith element (i = 1, 2,..., m, m denotes the sum of elements). To model the flexible plate, the mass matrix $[\boldsymbol{M}]$ and stiffness matrix $[\boldsymbol{K}]$ under global coordinate system (coordinate uvw) need to be found first. In fact, they can be constructed by the element matrixes.

Assume that $\{\boldsymbol{x}\} = \{x_1\ x_2\ \ldots\ x_n\}^{\mathrm{T}}$ is the displacement vector under global coordinate system (also calls global displacement vector), where n = 12m is the number of DOFs of the system; we also assume $\{\boldsymbol{\delta}^{ei}\}$ is the displacement vector of the ith element under the ith local coordinate system (also calls local displacement vector). Then we can get the relationship between $\{\boldsymbol{x}\}$ and $\{\boldsymbol{\delta}^{ei}\}$:

$$\{\boldsymbol{x}\} = [\boldsymbol{R}^{ei}]\{\boldsymbol{\delta}^{ei}\}, \tag{1}$$

where $[\boldsymbol{R}^{ei}]$ is a (12m × 12)-dimensional relation matrix, which can be used to deduce $[\boldsymbol{M}]$ and $[\boldsymbol{K}]$ from $[\boldsymbol{M}^{ei}]$ and $[\boldsymbol{K}^{ei}]$:

$$\begin{aligned}[\boldsymbol{M}] &= \sum_{i=1}^{\mathrm{m}}[\boldsymbol{R}^{ei}][\boldsymbol{M}^{ei}][\boldsymbol{R}^{ei}]^{\mathrm{T}},\\ [\boldsymbol{K}] &= \sum_{i=1}^{\mathrm{m}}[\boldsymbol{R}^{ei}][\boldsymbol{K}^{ei}][\boldsymbol{R}^{ei}]^{\mathrm{T}},\end{aligned} \tag{2}$$

where both $[\boldsymbol{M}]$ and $[\boldsymbol{K}]$ are (12m × 12m)-dimensional matrixes.

2.2 Modal analysis

The purpose of the modal analysis is to transfer the linear time-invariant vibration equations from the physical coordinate to the modal coordinate to make them decoupled. Since the flexible plate system is a distributed parameter system, it can be dispersed in space to get the following discrete vibration equation:

$$[\boldsymbol{M}]\{\ddot{\boldsymbol{x}}\} + [\boldsymbol{K}]\{\boldsymbol{x}\} = \{\boldsymbol{F}\}, \tag{3}$$

where $\{\boldsymbol{x}\}$ is the global displacement vector, containing a linear displacement and two angular displacement; $\{\ddot{\boldsymbol{x}}\}$ is the global acceleration vector, containing a linear acceleration and two angular acceleration; $\{\boldsymbol{F}\}$ is the global excitation force vector, containing a force and two moments; $[\boldsymbol{M}]$ and $[\boldsymbol{K}]$ have the same definition as Eq. (2).

To analyze the forced vibration of the system, the nature vibration should be solved first to get the nature frequency and modal of vibration. Let's wipe the excitation force off, so the nature vibration equation of system is

$$[\boldsymbol{M}]\{\ddot{\boldsymbol{x}}\} + [\boldsymbol{K}]\{\boldsymbol{x}\} = \boldsymbol{0}. \tag{4}$$

Let the general solution of the equation be $\{\boldsymbol{\Phi}\}\sin(\omega t + \varphi)$, substitute it back to Eq. (4) to get the modal equation:

$$([\boldsymbol{K}] - \omega^2[\boldsymbol{M}])\{\boldsymbol{\Phi}\} = \boldsymbol{0}, \tag{5}$$

where $[\boldsymbol{K}] - \omega^2[\boldsymbol{M}]$ is the eigenmatrix, ω is the eigenvalue,

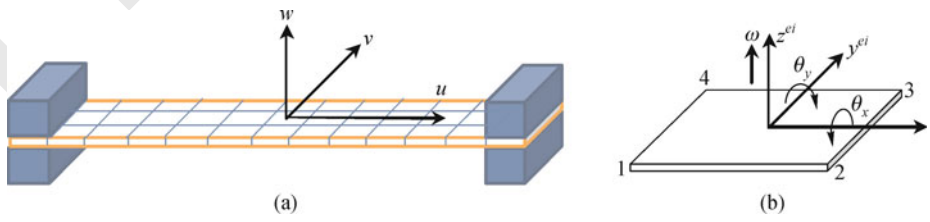

Fig. 1 Finite element model of the simply supported plate. (a) Element division of the plate under the global coordinate system uvw; (b) DOFs of the ith element under the local coordinate system $x^{ei}y^{ei}z^{ei}$

$\{\boldsymbol{\Phi}\}$ is the eigenvector. To solve Eq. (5), we let the determinant of eigenmatrix to be zero, i.e.,

$$\det([\boldsymbol{K}]-\omega^2[\boldsymbol{M}])=0. \tag{6}$$

To an n DOFs positive definite system, it exists n different nontrivial eigenvalues, which are all gathered and ordered into eigenvalue vector $\{\boldsymbol{\omega}\}=\{\omega_1\ \omega_2\ldots\ \omega_n\}$. ω is sorted by ascending order and ω_i ($i=1,2,\ldots,n$) is called the ith eigenvector, indicating the ith nature frequency. The corresponding eigenvectors are also gathered and sorted into the modal matrix $[\boldsymbol{\Phi}]=[\{\boldsymbol{\Phi}_1\}\{\boldsymbol{\Phi}_2\}\ldots\{\boldsymbol{\Phi}_n\}]$. By pre-multiplying each term of the forced vibration equation $[\boldsymbol{\Phi}]^{\mathrm{T}}$, Eq. (3) can be decoupled. Let the terms under modal coordinate system and that under physical coordinate system have the following relationships:

$$\begin{aligned}\{\boldsymbol{x}\}&=[\boldsymbol{\Phi}]\{\boldsymbol{\eta}\},\\ [\boldsymbol{M}_p]&=[\boldsymbol{\Phi}]^{\mathrm{T}}[\boldsymbol{M}][\boldsymbol{\Phi}],\\ [\boldsymbol{K}_p]&=[\boldsymbol{\Phi}]^{\mathrm{T}}[\boldsymbol{K}][\boldsymbol{\Phi}].\end{aligned} \tag{7}$$

Then, the decoupled modal equation is written as

$$[\boldsymbol{M}_p]\{\ddot{\boldsymbol{\eta}}\}+[\boldsymbol{K}_p]\{\boldsymbol{\eta}\}=[\boldsymbol{\Phi}]^{\mathrm{T}}\{\boldsymbol{F}\}, \tag{8}$$

where $\{\ddot{\boldsymbol{\eta}}\}$ and $\{\boldsymbol{\eta}\}$ are the acceleration and the displacement under modal coordinate system. $[\boldsymbol{M}_p]$ and $[\boldsymbol{K}_p]$ are the decoupled mass matrix and the decoupled stiffness matrix (diagonal matrixes).

Solving Eq. (8), the displacements under modal coordinate system, which is the linear superposition of the excitation force, is

$$\eta_j=\sum_{r=1}^{n}\frac{\varphi_{rj}F_r(\omega_r t)}{k_{jj}-m_{jj}\omega_r^2}, \tag{9}$$

where $j=1,2,\ldots,$n, is the number of nodes. n = 12m is the whole DOFs of the system. φ, k, m are elements of the modal matrix $[\boldsymbol{\Phi}]^{\mathrm{T}}$, the decoupled stiffness matrix $[\boldsymbol{K}_p]$ and the decoupled mass matrix $[\boldsymbol{M}_p]$ respectively (subscripts indicate the location in the matrix). $F_r(\omega_r t)$ is the element of excitation vector $\{\boldsymbol{F}\}$.

Since the displacement under the physical coordinate and the modal coordinate have the relationship as Eq. (8), the vibration equation under the physical coordinate can be solved.

Through the FEM analysis and the modal analysis, the modeling of the forced vibration plate is achieved.

3 Algorithm

3.1 Frequency domain control scheme

The typical internal model feedback control scheme was applied for the active control. It consisted of a neural network identifier (NNI), a neural network controller (NNC), a "F → T" element, a "T → F" element, "Sampling" elements (works only in experiments) and a feedback gain, as shown in Fig. 2. NNI, which learns from the controlled system, here is the internal model of the control system. NNC that varies to adjust the control system is the most important and essential part of the system. "F → T" element, standing for frequency domain to time domain, here is a component that transfers output of NNC (the values of amplitude) into a signal sequence to excite the plate. On the other hand, "T → F" element, standing for time domain to frequency domain, is an element waiting to collect a signal sequence and then transfer it into frequency domain by fast fourier transform. In simulation, the controlled system means the finite element model. Since it is discrete itself, so there are no "Sampling" elements. For the experiment, the controlled system is a continuous system (the real plate), so we need sampling to the get discrete input and output signals. The feedback gain element is usually a constant representing the gain of feedback signal.

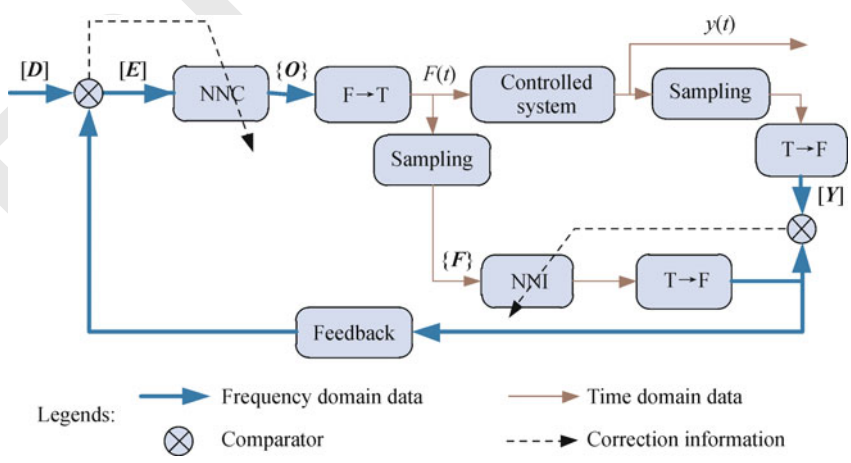

Fig. 2 Schematic diagram of the system. NNC: neural network controller; NNI: neural network identifier; F → T: frequency domain to time domain; T → F: time domain to frequency domain

3.2 Controller and identifier

The controller is a three layer back-propagation (BP) neural network, as shown in Fig. 3. It has an input layer with i neurons, a hidden layer with j neurons and an output layer with k neurons. The input vector $\{\boldsymbol{E}\}$, the hidden vector $\{\boldsymbol{H}\}$ and the output vector $\{\boldsymbol{O}\}$ are consisted of the value of input layer neurons, the value of hidden layer neurons and that of output layer neurons, respectively. $\{\boldsymbol{A}\}$ and $\{\boldsymbol{B}\}$ are the threshold of hidden layer and output layer. $\{\boldsymbol{D}\}$ is the target vector, which has the same dimension with $\{\boldsymbol{O}\}$. From the input layer to the output layer, the network has the following forward path relationships:

$$\begin{aligned}\{\boldsymbol{H}\} &= f([\boldsymbol{W}]\{\boldsymbol{E}\}-\{\boldsymbol{A}\}),\\ \{\boldsymbol{O}\} &= g([\boldsymbol{V}]\{\boldsymbol{H}\}-\{\boldsymbol{B}\}),\end{aligned} \tag{10}$$

where $[\boldsymbol{W}]$ is the $(j \times i)$-dimensional hidden layer weight matrix, while $[\boldsymbol{V}]$ is the $(k \times j)$-dimensional output layer weight matrix. The hidden layer excitation function is sigmoid function (also calls sigmoid neuron) $f(x) = 1/(1 + e^{-x})$, which is a bounded input/bounded output function, while the output layer excitation function is linear function (also calls linear neuron) $g(x) = x$. In fact, the input layer neurons, which are tapping points, can also be regarded as linear neurons.

The identifier is a two layered linear neural network, as shown in Fig. 4. Sampling the excitation force $\boldsymbol{F}(t)$ to get the input vector of NNI $\{\boldsymbol{F}\}$. The output of NNI $\{\hat{\boldsymbol{Y}}\}$ is an approximation of the real system output $\{\boldsymbol{Y}\}$. The NNI has the following relationship:

$$\{\hat{\boldsymbol{Y}}\} = [\boldsymbol{U}]\{\boldsymbol{F}\}, \tag{11}$$

where $[\boldsymbol{U}]$ is a $(n \times i)$-dimensional identifier weight matrix, which is continuously updating to insure that $\{\hat{\boldsymbol{Y}}\}$ and $\{\boldsymbol{Y}\}$ are closely approximative.

How the "F → T" element works? Let's get start with a two dimensional NNC output vector. Assuming that:

$$\{\boldsymbol{F}\} = [\boldsymbol{S}]\{\boldsymbol{O}\}, \tag{12}$$

where $[\boldsymbol{S}]$ denotes the relation matrix between $\{\boldsymbol{O}\}$ and $\{\boldsymbol{F}\}$. For a two dimension NNC output $\{\boldsymbol{O}\} = \{o_1\ o_2\}^{\mathrm{T}}$, it contains the amplitude values of two sine signals. Since $\{\boldsymbol{F}\}=\{F_1\ \ F_2\}^{\mathrm{T}}=\{A_1\sin(\omega_1 t)\ \ A_2\sin(\omega_2 t)\}^{\mathrm{T}}$, the "F → T" element can be written as

$$\begin{bmatrix} F_1 \\ F_2 \end{bmatrix} = \begin{bmatrix} \sin(\omega_1 t) & 0 \\ 0 & \sin(\omega_2 t) \end{bmatrix} \begin{bmatrix} A_1 \\ A_2 \end{bmatrix}. \tag{13}$$

As we will conduct the algorithm in frequency domain, an input signal sequence to the system needs first. So the outputs of the "F → T" element are sampled. We consider the length of the sampling point is i. Then Eq. (13) is written as

$$\begin{bmatrix} F_{11} \\ \vdots \\ F_{1i} \\ F_{21} \\ \vdots \\ F_{2i} \end{bmatrix} = \begin{bmatrix} \sin(\omega_1 t_1) & 0 \\ \vdots & \vdots \\ \sin(\omega_1 t_i) & 0 \\ 0 & \sin(\omega_2 t_1) \\ \vdots & \vdots \\ 0 & \sin(\omega_2 t_i) \end{bmatrix} \begin{bmatrix} A_1 \\ A_2 \end{bmatrix}. \tag{14}$$

On the other hand, the "T → F" element is implemented by fast fourier transform.

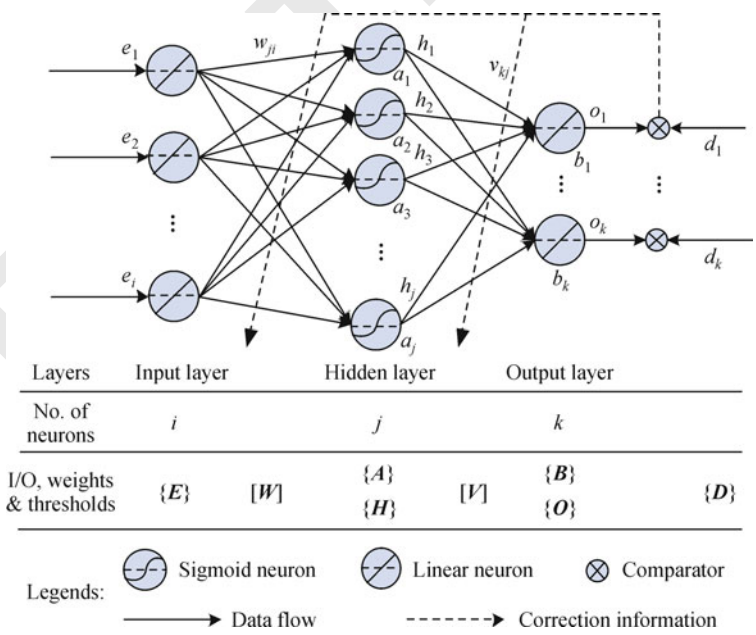

Fig. 3 Architecture of neural network controller

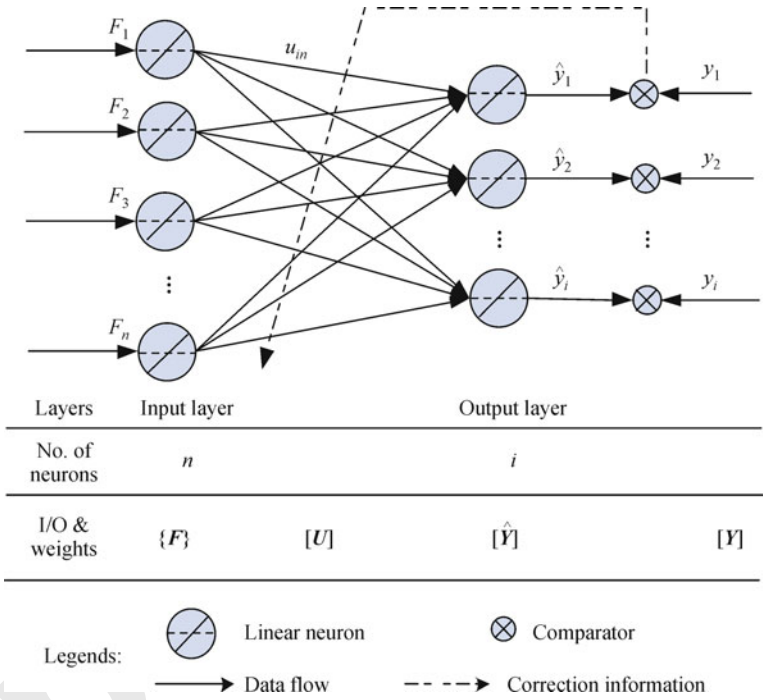

Fig. 4 Architecture of neural network identifier

3.3 Back propagation law

The gradient decent method is used for error correction. The target function of the system defines as follows:

$$J = \frac{1}{2}\sum_i (d_i - y_i)^2, \tag{15}$$

where y_i is the element of output vector $\{\boldsymbol{Y}\}$, d_i is the element of target vector $\{\boldsymbol{D}\}$.

The error function is actually the variance of the output vector and target vector. What need to be update in NNC to minimum the target function are the hidden layer weight matrix $[\boldsymbol{W}]$, the hidden layer threshold vector $\{\boldsymbol{A}\}$, the output layer weight matrix $[\boldsymbol{V}]$ and the output layer threshold vector $\{\boldsymbol{B}\}$. From Eqs. (10) to Eq. (15), it can be seen that the error J is a function of these matrixes or vectors, i.e., $J = h([\boldsymbol{V}], \{\boldsymbol{B}\}, [\boldsymbol{W}], \{\boldsymbol{A}\})$. Using the chain derivation method of compound function and the gradient decent method, the updating value of each step of these matrixes or vectors are

$$\begin{aligned} [\Delta \boldsymbol{V}] &= -\eta \frac{\partial J}{\partial [\boldsymbol{V}]}, \\ [\Delta \boldsymbol{B}] &= -\eta \frac{\partial J}{\partial [\boldsymbol{B}]}, \\ [\Delta \boldsymbol{W}] &= -\eta \frac{\partial J}{\partial [\boldsymbol{W}]}, \\ [\Delta \boldsymbol{A}] &= -\eta \frac{\partial J}{\partial [\boldsymbol{A}]}, \end{aligned} \tag{16}$$

where η denotes the coefficient of convergence.

3.4 Simulation

The NNC was programmed as a main program, while FEM and NNI were programmed as subprograms. It called subprograms in main program and kept updating the weights and thresholds until the target function (also called the error) becomes small enough. The flow diagram of the control system is shown in Fig. 5.

The number of the input layer neurons was chosen as 1000, the number of hidden layer neurons was chosen as 67 and that of output layer neurons was chosen as 2. In that case, the length of feedback signal is 1000 sampling points in time domain (the sampling frequency is 1000 Hz), the length of the input layer of the identifier is 2000 and that of the output layer of the identifier is 1000. The target spectrum peak was set at 10 and 20 Hz and the target error was chosen as $J_{\text{tar}} = 10^{-4}$. The simulation result showed that the control system perform perfectly as shown in Figs. 6 and 7.

Figure 6 shows the simulation results when the coefficient of convergence $\eta = 0.1$. The amplitude of the controlled spectrum (Fig. 6(b)) is almost equal to the amplitude of the target spectrum (Fig. 6(a)). The error curve (Fig. 6(c)) declines exponentially. Since the coefficient of convergence is large, the error curve vibrates, so does the amplitude of the 10 and 20 Hz components (Figs. 6(d) and 6(e)). The whole learning process ends within 50 iterations. In Fig. 7, the coefficient of convergence is changed to $\eta = 0.01$. The controlled spectrum also matches the target perfectly. The error curve and amplitude changes of components become smooth, but the iterations increase to 1000.

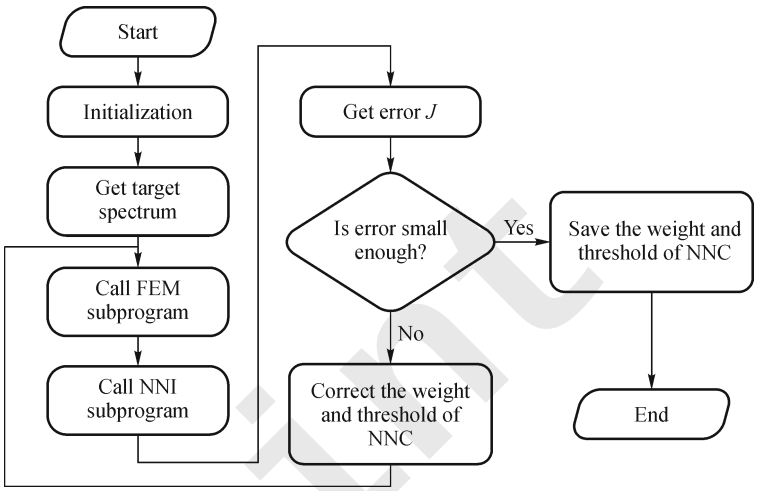

Fig. 5 Flow diagram of the control system

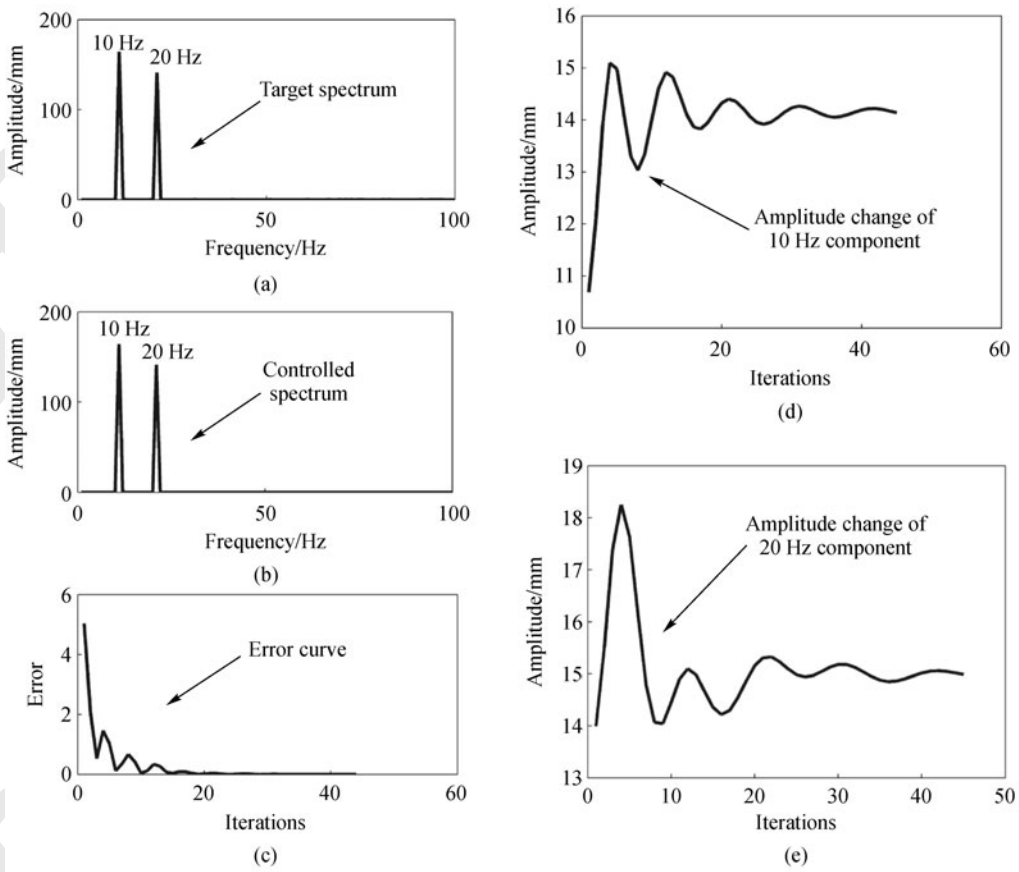

Fig. 6 Simulation result when $\eta = 0.1$. (a) Target spectrum; (b) controlled spectrum; (c) error curve; (d) time domain amplitude of 10 Hz component; (e) time domain amplitude of 20 Hz component

4 Pre-testing experiment

The scheme of the experiment system is shown in Fig. 8. Sensors collect signals from the vibrating plate and send them into the industrial personal computer (IPC) through data acquisition instrument. Then the processed signals are sent out from the IPC to excite the plate through amplifier.

The type of sensors is 352C34. They are a kind of

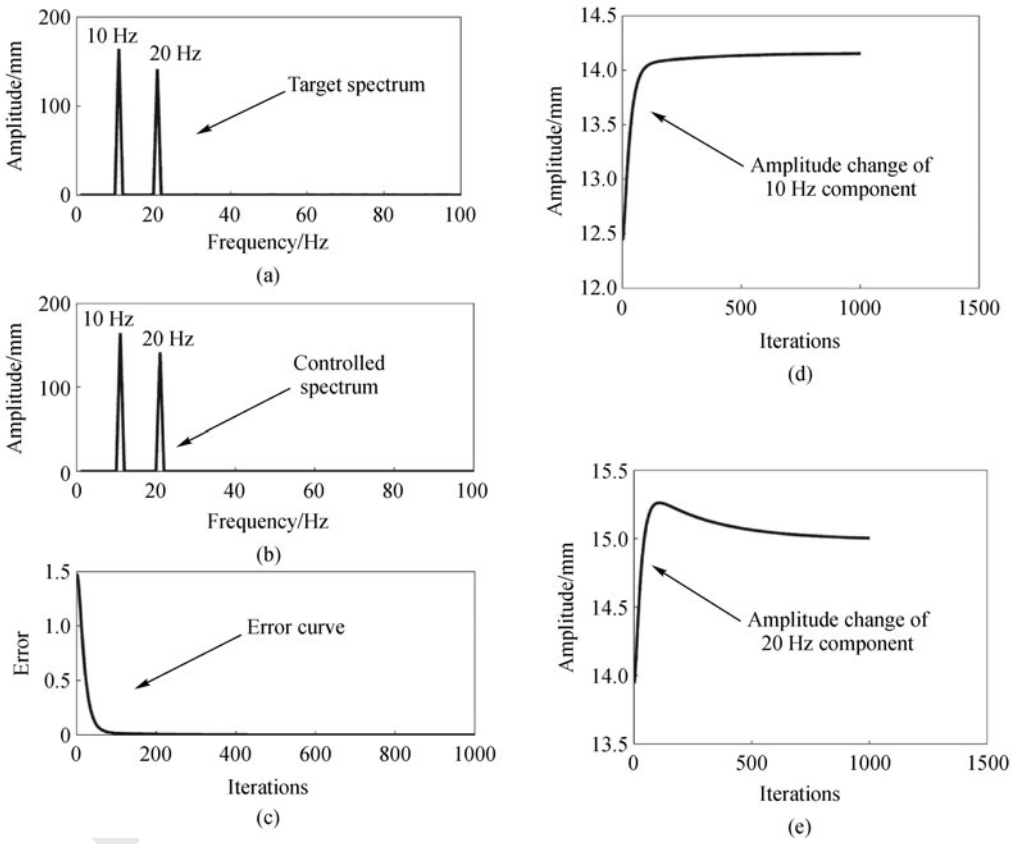

Fig. 7 Simulation result when $\eta = 0.01$. (a) Target spectrum; (b) controlled spectrum; (c) error curve; (d) time domain amplitude of 10 Hz component; (e) time domain amplitude of 20 Hz component

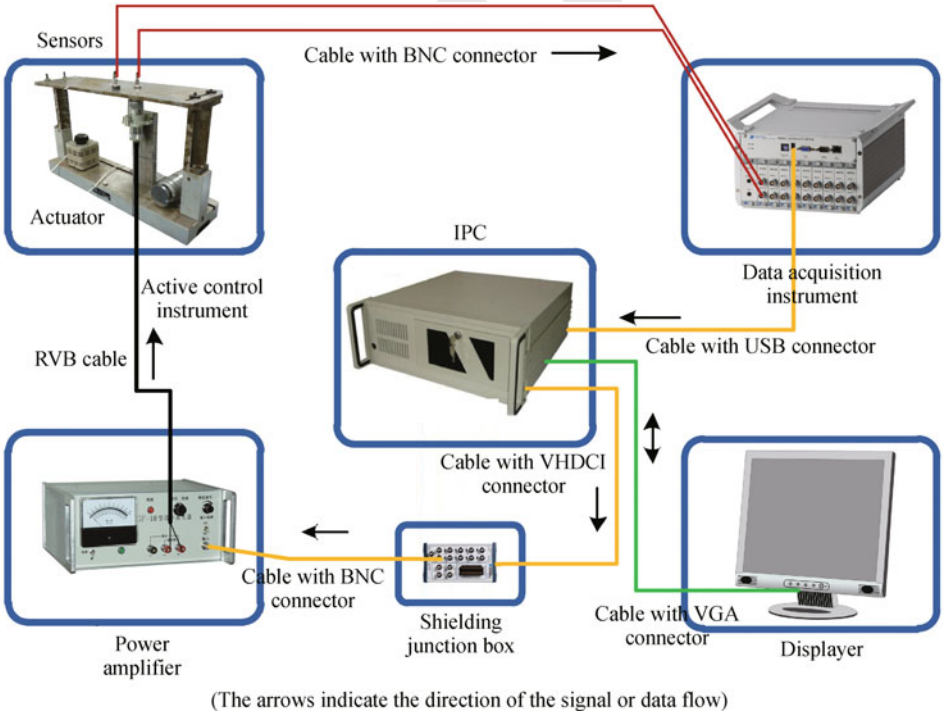

Fig. 8 Structure of the experiment system (notes: IPC stands for industrial personal computer; RVB stands for red vs blue; USB stands for universal serial bus; BNC stands for bayonet nut connector; VHDCI stands for very high density cable interconnect; VGA stands for video graphic array)

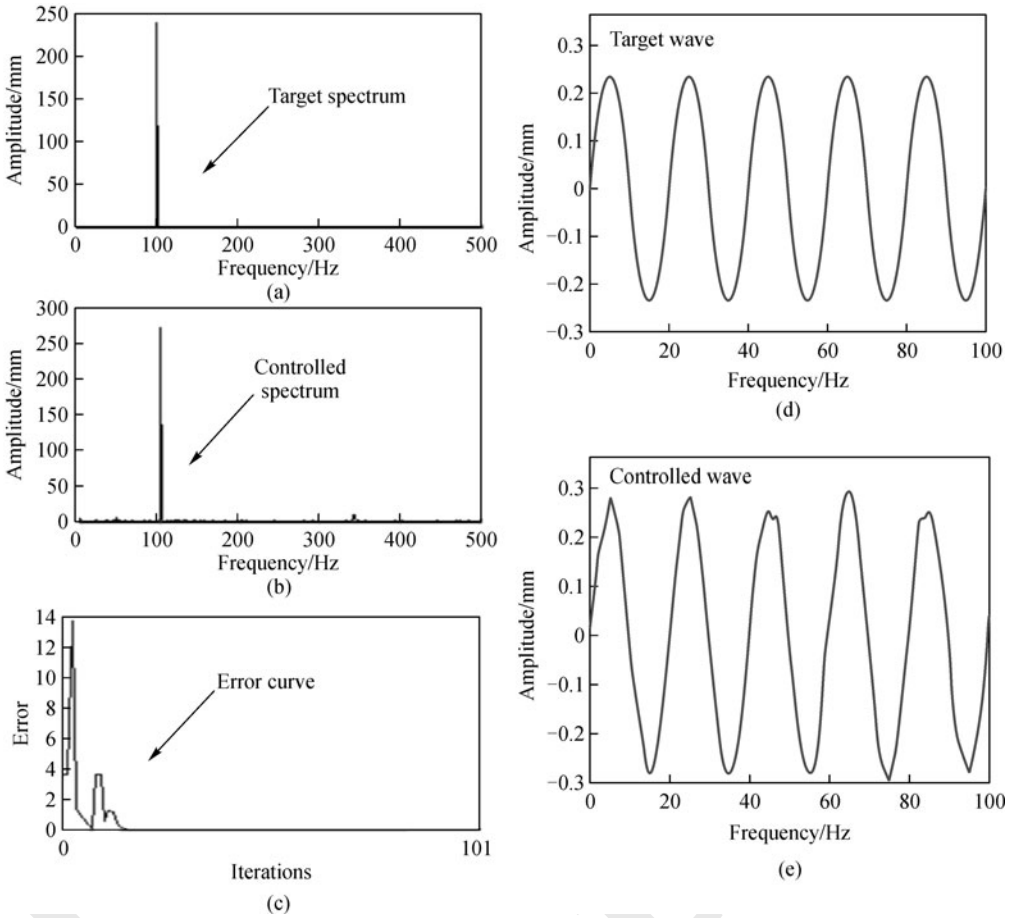

Fig. 9 Result of the pre-testing experiment. (a) Target spectrum; (b) controlled spectrum; (c) error curve; (d) target wave; (e) controlled wave

piezoelectric ceramics acceleration sensors made by PCB Company, USA. The type of data acquisition instrument is YE2326 from Sinocera Piezotronics Inc, China. The IPC have equipped with the PCI6221 data acquisition card from NI Company, USA. The type of actuator is JZ-1 made by Far East Corporation, Beijing, China, and the type of power amplifier is GF-10 made by Far East Corporation, Beijing, China. The experiment was conducted by the software LABVIEW.

The pre-testing experiment was an exploratory activity upon this algorithm, so only the one-frequency-point control was achieved. Some primary results were concluded through the pre-testing, they are

1) The correctness of algorithm was verified by implementing it on real system.

2) Sine input (Fig. 9(d)) did not get the perfect sine output (Fig. 9(e)) due to the noise. That is what made the control difficult.

3) The amplitude of the target and controlled wave ranged from 0.2 to 0.3 mm, indicating that the control aim achieved.

4) The error line declined almost exponentially.

5 Conclusions

A NN-based adaptive control algorithm for active control, which was conducted in frequency domain, was proposed. Multi-frequency control was achieved in simulation. The pre-testing experiment of the algorithm on real vibration system was implemented. The result of the simulation shows that the amplitudes of some certain frequency points can be easily positioned and controlled by frequency domain control and the system can reject noise or disturbance easier by the intelligent NN method. The pre-testing experiment verified the correctness of the algorithm. However, the work needs go further, especially the experimental investigations. We hope that this advanced control method could finally be realized and this work could lay foundations for the active control of mechanical structures.

Acknowledgements This work was supported by the National Natural Science Foundation of China (Grant Nos. 51225501 and 51175401) and the Program for Changjiang Scholars and Innovative Research Team in University.

References

1. Hu Z W. A review of active vibration control for structures. Journal of Mechanical Strength, 1995, 17(2): 55–60 (in Chinese)
2. Lane S A, Clark R L, Southward S C. Active control of low frequency modes in an aircraft fuselage using spatially weighted arrays. Journal of Vibration and Acoustics-Transactions of the ASME, 2000, 122(3): 227–234
3. de Klerk D, Ossipov A. Operational transfer path analysis: theory, guidelines and tire noise application. Mechanical Systems and Signal Processing, 2010, 24(7): 1950–1962
4. Alavinasab A, Moharrami H, Khajepour A. Active control of structures using energy-based LQR method. Computer-Aided Civil and Infrastructure Engineering, 2006, 21(8): 605–611
5. Zhang J J, He L L, Wang E C, Gao R E. The design of LQR controller based on independent mode space for active vibration control. Advances in Computation and Intelligence, 2008, 5370: 649–658
6. Gao H J, Sun W C, Shi P. Robust sampled-data H_∞ control for vehicle active suspension systems. IEEE Transactions on Control Systems Technology, 2010, 18(1): 238–245
7. Moheimani S, Vautier B, Bhikkaji B. Experimental implementation of extended multivariable PPF control on an active structure. IEEE Transactions on Control Systems Technology, 2006, 14(3): 443–455
8. Rao V, Damle R, Tebbe C, Kern F. The adaptive control of smart structures using neural networks. Smart Materials and Structures, 1994, 3(3): 354–366
9. Damle R, Lashlee R, Rao V, Kern F. Identification and robust control of smart structures using artificial neural networks. Smart Materials and Structures, 1994, 3(1): 35–46
10. Damle R, Rao V, Kern F. Robust control of smart structures using neural network hardware. Smart Materials and Structures, 1997, 6 (3): 301–314
11. Jha R, He C L. Neural-network-based adaptive predictive control for vibration suppression of smart structures. Smart Materials and Structures, 2002, 11(6): 909–916
12. Jnifene A, Andrews W. Experimental study on active vibration control of a single-link flexible manipulator using tools of fuzzy logic and neural networks. IEEE Transactions on Instrumentation and Measurement, 2005, 54(3): 1200–1208
13. Kumar R, Singh S P, Chandrawat H N. MIMO adaptive vibration control of smart structures with quickly varying parameters: neural networks vs classical control approach. Journal of Sound and Vibration, 2007, 307(3–5): 639–661
14. Madkour A, Hossain M A, Dahal K P, Yu H. Intelligent learning algorithms for active vibration control. IEEE Transactions on Systems, Man, and Cybernetics, Part C: Applications and Reviews, 2007, 37(5): 1022–1033
15. Abiyev R H, Kaynak O. Fuzzy wavelet neural networks for identification and control of dynamic plants – a novel structure and a comparative study. IEEE Transactions on Industrial Electronics, 2008, 55(8): 3133–3140
16. Pan Y P, Wang J. Model predictive control of unknown nonlinear dynamical systems based on recurrent neural networks. IEEE Transactions on Industrial Electronics, 2012, 59(8): 3089–3101
17. Zhang X W, Chen X F, You S Q, He Z, Li B. Simulation and experimental investigation of structural dynamic frequency characteristics control. Sensors (Basel, Switzerland), 2012, 12(4): 4986–5004